IEEE Access
Multidisciplinary | Rapid Review | Open Access Journal

Received June 2, 2019, accepted June 14, 2019, date of publication June 19, 2019, date of current version July 3, 2019.

Digital Object Identifier 10.1109/ACCESS.2019.2923683

Linear Constellation Precoded OFDM With Interleaved Subcarrier Index Modulation

QINGBO WANG, GAOQI DOU, JUN GAO, AND RAN DENG
Department of Communication Engineering, Naval University of Engineering, Wuhan 430033, China

Corresponding author: Gaoqi Dou (hjgcqq@163.com)

This work was supported by the National Natural Science Foundation of China (NSFC) under Grant 61871473.

ABSTRACT Orthogonal frequency-division multiplexing with index modulation (OFDM-IM) is an emerging and promising multicarrier transmission technique; however, frequency diversity achievement requires further investigation for the OFDM-IM. In this paper, the linear constellation precoded OFDM with interleaved subcarrier index modulation (LCP-OFDM-ISIM) is proposed, where a unitary matrix is employed to spread the constellation symbols over all the active subcarriers of the block and the binary constant weight code (BCWC) is utilized as the subcarrier activation pattern (SAP). At the receiver, energy detection is employed to initialize the SAP estimation, and then, the cascaded feedback detection is proposed to refine the detection performance by passing the detection results between the symbol detection and the data-assisted SAP detection. For L-taps channel, conditioned on the BCWC with the minimum Hamming distance of d, energy detection can achieve the diversity order of $\min(d/2, r)$, and a closed-form expression is derived for the energy detection. It is shown, via the pair-wise error probability, that the data-assisted SAP detection included in cascaded feedback detection can achieve the diversity order of $\min(d, L)$. The simulation results are provided to show the superiority of the LCP-OFDM-ISIM over the benchmarks.

INDEX TERMS Orthogonal frequency division multiplexing, index modulation, linear constellation precoding, frequency diversity.

I. INTRODUCTION

Orthogonal frequency division multiplexing with index modulation (OFDM-IM) [1] activates part of the subcarriers to convey the constellation symbols, the subcarrier activation patterns (SAPs) are also exploited to convey additional information. Due to its favorable power consumption property, the OFDM-IM achieves an interesting trade-off between spectral efficiency (SE) and energy efficiency (EE), which inspires many researchers to explore its potential to meet the challenging objectives of future wireless networks [2], [3]. The interested readers can refer to [4] for the survey of IM.

However, the SE of the OFDM-IM is limited, since the inactive subcarriers do not convey the constellation symbols. To improve the SE, several enhanced OFDM-IM schemes have been proposed, such as the OFDM with generalized index modulation (OFDM-GIM) [5], OFDM with hybrid in-phase/ quadrature IM (OFDM-HIQ-IM) [6], dual-mode OFDM-IM (DM-OFDM-IM) [7], and multiple-mode OFDM-IM (MM-OFDM-IM) [8]. Moreover, in [9], the principle of IM is extended to multidomain, the compressed-sensing-aided space-time frequency IM was proposed for the multiple-input multiple-output system. Further, non-coherent OFDM-IM [10] and OFDM with differential subcarrier index modulation (OFDM-DSIM) [11] have been proposed, to avoid the consumption of transmission resources for channel estimation.

On the other hand, to improve the performance of the OFDM-IM under the mutipath Rayleigh channel, many schemes have been proposed to exploit the frequency diversity to combat the frequency-selective fading. In [12], OFDM with interleaved subcarrier IM (OFDM-ISIM) was proposed to improve the performance by enlarging the Euclidean distance of the modulated symbols. As shown in this paper, OFDM-ISIM in [12] achieves the diversity order of two for the information conveyed by the SAPs, however, the diversity is absent for the information conveyed by the constellation symbols. In [13], coordinate interleaved OFDM-IM (CI-OFDM-IM) was proposed, where the real and imaginary part of the complex symbols are transmitted over different

The associate editor coordinating the review of this manuscript and approving it for publication was Cunhua Pan.

active subcarriers. However, the maximum achievable diversity order is just two for the CI-OFDM-IM. To achieve higher diversity order, enhanced CI-OFDM-IM (ECI-OFDM-IM) was proposed in [14], where the CI is performed twice for four complex symbols to achieve the diversity order of four. However, the ECI is no longer an orthogonal design, the diversity is achieved at the cost of the Euclidean distance between the symbols. In [15], coded OFDM-IM with transmit diversity was proposed, where the same SAP is used for several groups, the diversity is achieved at the cost of SE, however the achievable diversity order was not provided. In essence, the method proposed in [15] is equivalent to using the repetition code as the SAP, and the repetition code can be regarded as a special binary constant weight code (BCWC), utilized in this paper.

In [6] and [8], linear precoding (LP) was respectively considered for OFDM-IM-IQ and MM-OFDM-IM-IQ, to achieve the diversity order of two without the loss of SE. In [16], spread OFDM-IM (S-OFDM-IM) was proposed, where both the non-zero constellation symbols and SAP are spread and compressed into all the subcarriers of a group, to achieve the diversity. In [17], linear precoded IM (LPIM) was proposed to achieve the diversity by the design of LPIM codebook. Further, to avoid the huge complexity, a low complexity generalized iterative residual check detector (GIRCD) was proposed. However both S-OFDM-IM and LPIM scheme spread the constellation symbols over all the subcarriers of a group, the inactive subcarriers are no longer zero-valued, which hinders the utilization of the zero-valued inactive subcarriers in the OFDM-IM, such as in [18], the zero-valued inactive subcarriers were exploited to refine the carrier frequency offset (CFO) estimation for the OFDM-GIM.

As shown in above, frequency diversity achievement requires further investigation for the OFDM-IM. In this paper, we focus on the frequency diversity achievement, linear constellation precoded OFDM with ISIM (LCP-OFDM-ISIM) is proposed. The main contributions of this paper are summarized as follows:

(i) The LCP-OFDM-ISIM is proposed, where a unitary matrix is used to spread the constellation symbols over all the active subcarriers of the block, and BCWC is utilized as the SAP. Since the constellation symbols are spread over all the active subcarriers of the block, rather than all the subcarriers (the active and inactive) of a group like in [16], [17], the diversity can be achieved for the information conveyed by the constellation symbols, meanwhile, the inactive subcarriers are still zero-valued in the proposed LCP-OFDM-ISIM.

(ii) Since the constellation symbols are spread over all the active subcarriers of the block, rather than all the subcarriers of a group, the existing maximum likelihood (ML) and log-likelihood ratio (LLR) detection are no longer feasible for the LCP-OFDM-ISIM, which will be detailed in section II. At the receiver, we first resort to the simple energy detection to initialize the SAP estimation, then the cascaded feedback detection is proposed to improve the detection performance of both the constellation symbols and SAPs, by passing the detection results between the symbol detection and data-assisted SAP detection.

(iii) The BCWC is utilized as the SAP to achieve the diversity for the information conveyed by the SAPs. Although the BCWC with the minimum Hamming distance of four, was employed in the ECI-OFDM-IM [14], in this paper, the diversity of the information conveyed by the SAPs, is analyzed in detail. Energy detection can achieve the diversity order of $min(d/2, L)$ and a closed-form expression is derived for the energy detection, it is shown via the pair-wise error probability (PEP) analysis that the data-assisted SAP detection can achieve the diversity order of $min(d, L)$ for L-taps channel, conditioned on the BCWC with the minimum Hamming distance of d. Further, the transmit diversity scheme proposed in [15] is equivalent to using repetition code as the SAP, the repetition code can be regarded as a special BCWC, utilized in this paper.

The rest of this paper is organized as follows. The system model of the LCP-OFDM-ISIM is presented in Section II. In Section III, the diversity order of energy detection and data-assisted SAP detection is analyzed. Section IV presents the simulation results. Finally, the paper is concluded in Section V.

Notation: Boldface small and capital letters stand for vectors and matrices, respectively. Hermitian transpose, transpose, complex conjugate and inverse are denoted by $(\cdot)^H$, $(\cdot)^T$, $(\cdot)^*$ and $(\cdot)^{-1}$, respectively. $E\{\cdot\}$ denotes the statistical expectation. $\|\cdot\|_2$ and $|\cdot|$ denote the 2-norm and absolute. $n!$ denotes the factorial of n. $\mathcal{C}(n, k)$ denotes the binomial coefficient. $\lfloor\cdot\rfloor$ denotes the floor function. The $N \times N$ energy-preserving discrete Fourier transform (DFT) matrix is defined as $\mathbf{F}_N(n, m) = \frac{1}{\sqrt{N}} e^{-j2\pi nm/N}$, and $\mathbf{F}_L$ denotes the $N \times L$ sub-matrix obtained from the front L columns of $\mathbf{F}_N$.

II. SYSTEM MODEL OF THE LCP-OFDM-ISIM

The block diagram of the LCP-OFDM-ISIM is given in Fig. 1. The multipath Rayleigh channel is considered. Let $\mathbf{h}_\mathcal{T} \in \mathbb{C}^{L\times 1}$ denotes the baud-rate sampled discrete-time channel impulse response (CIR), where L is the channel order and $E\{\mathbf{h}_\mathcal{T}^T \mathbf{h}_\mathcal{T}\} = \frac{1}{L}\mathbf{I}_L$. The CIR is assumed to be known at the receiver, but unknown at the transmitter. The system is assumed to be perfectly synchronized and the sufficient cyclic prefix (CP) is appropriately added at the transmitter and removed at the receiver. Both the inter-symbol interference (ISI) and inter-carrier interference (ICI) are assumed to be completely suppressed.

A. TRANSMITTER

The OFDM block with N subcarriers is divided into G groups with n subcarriers, i.e., $Gn = N$. In each group, k out of n subcarriers are activated to convey the symbols, the SAPs are also exploited to convey additional information. To explain the principle of the OFDM-IM, a SAP selection example of look-up table method is provided in Table 1.

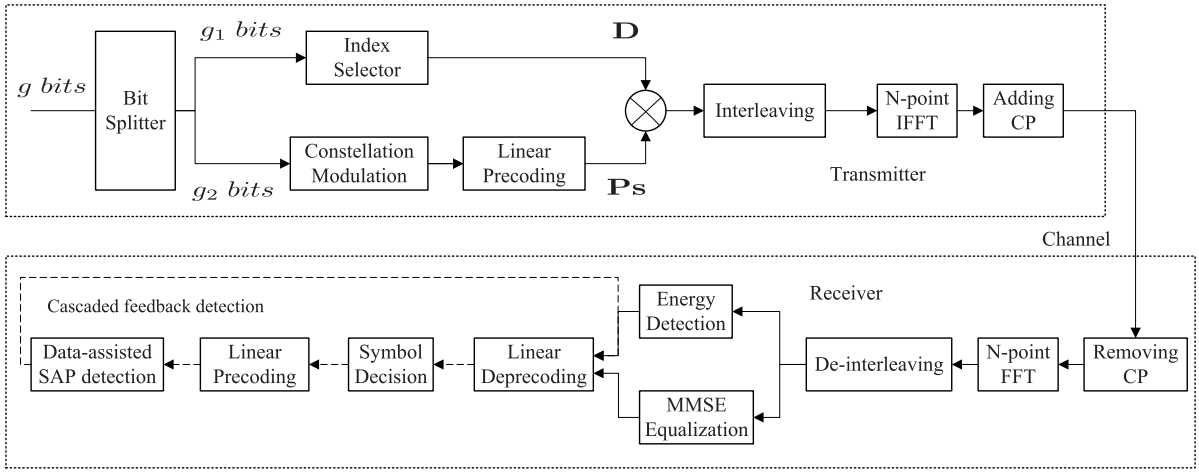

FIGURE 1. Block diagram of the proposed LCP-OFDM-ISIM.

TABLE 1. A look-up table example for (n, k) $\mathcal{D}$ $(8, 6)$, the BCWC $A(8, 4, 6)$ is adopted as the SAP.

Bits	Index of the active subcarriers ($\mathcal{A}$)	SAP ($\mathcal{I}$)	Group
[0 0]	[2 3 4 6 7 8]	[0 1 1 1 0 1 1 1]	[0 s_1 s_2 s_3 0 s_4 s_5 s_6]
[0 1]	[1 3 4 5 7 8]	[1 0 1 1 1 0 1 1]	[s_1 0 s_2 s_3 s_4 0 s_5 s_6]
[1 0]	[1 2 4 5 6 8]	[1 1 0 1 1 1 0 1]	[s_1 s_2 0 s_3 s_4 s_5 0 s_6]
[1 1]	[1 2 3 5 6 7]	[1 1 1 0 1 1 1 0]	[s_1 s_2 s_3 0 s_4 s_5 s_6 0]

In the LCP-OFDM-ISIM, the BCWC $A(n, d, k)$ is utilized as the SAP, where n is the length of binary code, which equals the group length, k is the code weight, namely, the number of the one-valued bits, which equals the number of the active subcarriers in each group, d is the minimum Hamming distance between two codes. If the tth bit of the BCWC is one-valued (zero-valued, respectively), the tth subcarrier is activated (inactivated, respectively). The details of BCWC is omitted here, the interested reader can refer to [19], [20] for the details.

In the coded OFDM-IM proposed in [15], the same SAP is used for several groups, which is called by a cluster, to achieve the diversity, at the cost of SE. In essence, the scheme proposed in [15] is equivalent to using the repetition code as the SAP for each cluster, and the repetition code is a special kind of BCWC. Generally, an appropriate BCWC can be chosen to achieve a higher SE in comparison with the repetition code. For example, as shown in this paper, to achieve the diversity order of four for the SAP for the LCP-OFDM-ISIM or the coded OFDM-IM proposed in [15], the minimum Hamming distance of SAP should be four at least. To achieve the minimum Hamming distance of four, if the repetition code is used as the SAP, the SAP in Table. 2 is obtained by repeating the SAP in Table. 3. However from the view point of BCWC, we can choose the SAP in Table. 1 as the SAP. Consequently, the OFDM-IM employing BPSK, achieves the SE of 1 bps/Hz and 0.75 bps/Hz for the Table. 1 and Table. 2, respectively.

TABLE 2. A look-up table example for (n, k) $\mathcal{D}$ $(4, 2)$, the repetition code is adopted as the SAP.

Bits	Index of the active subcarriers ($\mathcal{A}$)	SAP ($\mathcal{I}$)	Group
[0]	[1 3]	[1 0 1 0]	[s_1 0 s_2 0]
[1]	[2 4]	[0 1 0 1]	[0 s_1 0 s_2]

TABLE 3. A look-up table example for (n, k) $\mathcal{D}$ $(2, 1)$.

Bits	Index of the active subcarriers ($\mathcal{A}$)	SAP ($\mathcal{I}$)	Group
[0]	[1]	[1 0]	[s_1 0]
[1]	[2]	[0 1]	[0 s_1]

For the certain value of (n, d, k), the number of the BCWC $A(n, d, k)$ is limited. Hence, for a given the minimum Hamming distance between the SAPs d and the given value of (n, k), the number of the BCWC $A(n, d, k)$ may be insufficient to achieve the given SE. It is notable that we can enlarge the value of (n, k) to achieve the given SE and the minimum Hamming distance between the SAPs.

At the transmitter, the incoming $g = g_1 + g_2$ bits are split into two parts. The first $g_1 = G\lfloor \log_2 N_{\mathcal{I}} \rfloor$ bits are conveyed by the SAPs, where $N_{\mathcal{I}}$ denotes the number of the valid SAPs. Obviously, we have $N_{\mathcal{I}} \leq \log_2 \mathcal{C}(n, k)$. The remaining $g_2 = Gk \log_2 M$ bits are conveyed by the constellation symbols, where M is the modulation order.

The incoming $g_1 = G\lfloor \log_2 N_{\mathcal{I}} \rfloor$ bits are fed into the index selector, where the $G\lfloor \log_2 N_{\mathcal{I}} \rfloor$ bits are split into G subsequences with $\tilde{g}_1 = \lfloor \log_2 N_{\mathcal{I}} \rfloor$ bits, according to the provided look-up table, the tth subsequence with $\lfloor \log_2 N_{\mathcal{I}} \rfloor$ bits, is mapped to the SAP of the tth group, denoted by $\mathcal{I}^t$, $t \in [1, 2, \cdots, G]$, and the index of the active subcarriers is denoted by $\mathcal{A}^t$, which is a subset of $[1, \cdots, n]$, with cardinality k.

The index of the active subcarriers of the block is given by

$$\mathcal{A}_{block} = [\mathcal{A}^1, \mathcal{A}^2 + n, \cdots, \mathcal{A}^G + (G-1)n], \tag{1}$$

where $\mathcal{A}_{block}$ is a subset of $\{1, \cdots, N\}$, with cardinality $N_1 = Gk$. The data permutation matrix $\mathbf{D} \in \mathbb{C}^{N \times N_1}$, which is used to place the symbols on the active subcarriers, is generated as

$$\mathbf{D}(a,b) = \begin{cases} 1 & b = i, a = \mathcal{A}_{block}(i),\ \forall i \in \{1, 2, \cdots, N_1\}, \\ 0 & others. \end{cases} \tag{2}$$

The incoming $g_2 = Gk \log_2 M$ bits are mapped to the constellation symbol vector $\mathbf{s} \in \mathbb{C}^{N_1 \times 1}$. To achieve the frequency diversity, the LCP is performed, the constellation symbol vector $\mathbf{s}$ is multiplied by the precoder $\mathbf{P} \in \mathbb{C}^{N_1 \times N_1}$. Then, the signal is multiplied by the data permutation matrix $\mathbf{D}$, to place the elements of $\mathbf{Ps}$ on the active subcarriers one-by-one. The resulted signal is given by

$$\mathbf{x} = \gamma \mathbf{DPs}, \tag{3}$$

where $\gamma = \sqrt{n/k} = \sqrt{N/N_1}$ is the power compensation factor, which is used to normalize the average power of the signal. Noting that since the precoder is a square matrix and unitary, the Euclidean distance between any pairs of $\mathbf{s}$ is unchanged before and after the LCP.

Then the signal is interleaved by a matrix interleaver, where the elements of $\mathbf{x}$ are fed into a matrix row-by-row, and ejected column-by-column. After the N-point IFFT operation, addition of the CP, the signal is transmitted over the multipath channel.

B. RECEIVER

At the receiver, after removal of the CP, N-point FFT and de-interleaving, the received signal in the frequency domain is given by

$$\mathbf{y} = \gamma \mathbf{HDPs} + \mathbf{v}, \tag{4}$$

where $\mathbf{H}$ denotes the frequency-domain channel matrix after the de-interleaving, $\mathbf{v}$ is the additive white Gaussian noise (AWGN) with variance σ_v^2.

1) WHY THE EXISTING ML AND LLR DETECTION ARE NO LONGER FEASIBLE FOR THE LCP-OFDM-ISIM?

The ML detection and LLR detection have been proposed in [1]. The ML detection makes a joint decision on the constellation symbols and SAP. To reduce the computational complexity, the ML detection is performed group-by-group.

In the LCP-OFDM-ISIM, the elements of the signal are spread over all the active subcarriers of the block, the symbols on the active subcarriers in the block, rather than the symbols on the subcarriers of a group like in [16], [17], are correlated. The ML detection has to be performed on the whole block, instead of group-by-group. Hence for the LCP-OFDM-ISIM, the number of ML metric calculations, is $G2^{\tilde{g}_1}M^{Gk}$, rather than $G2^{\tilde{g}_1}M^k$ for the OFDM-IM in [1], [16], [17], which is too great to be practical and performable.

In the OFDM-IM, the symbols on the active subcarriers are from an finite set $\{0, \mathcal{S}\}$, where $\mathcal{S}$ denotes the set of constellation symbols. The LLR detection first calculates the LLR of the subcarrier is active to inactive, the SAP with the maximum LLR value is determined as the SAP for each group, then the corresponding constellation symbols are detected.

However, in the LCP-OFDM-ISIM, the elements of $\mathbf{s}$ are spread over all the active subcarriers, before the SAP detection, namely, when the active subcarriers are not determined, the linear deprecoding cannot be performed. Without the deprecoding, the symbols on the active subcarriers, i.e., the elements of $\mathbf{Ps}$, are different for the different realizations of $\mathbf{s}$, hence the symbol on the active subcarriers has the M^{Gk} different realizations, which makes the LLR calculation of each subcarrier be unpractical. Consequently, the LLR detection is infeasible for the LCP-OFDM-ISIM.

2) ENERGY DETECTION AND CASCADED FEEDBACK DETECTION

To make the detection of the LCP-OFDM-ISIM with performable computational complexity, the energy detection and cascaded feedback detection are proposed, where the simple energy detection is employed to initialize the SAP estimation, then the cascaded feedback detection is performed to refine the detection performance, by passing the detection results between the symbol detection and data-assisted SAP detection.

Before the cascaded feedback detection, the SAP estimation is initialized by energy detection, which determines the states (active or inactive) of the subcarriers by the signal energy, and the signal is equalized by a MMSE equalizer.

The MMSE equalization is given by

$$\bar{\mathbf{y}} = \Phi \mathbf{y}/\gamma, \tag{5}$$

where Φ is a diagonal matrix with the diagonal vector

$$\phi(i) = \frac{\mathbf{h}^*(i)}{|\mathbf{h}(i)|^2 + \sigma_v^2/\gamma^2}. \tag{6}$$

Noting that to simplify the iterative detection, the MMSE equalization is now performed for all the subcarriers.

Energy detection first calculates the energy of each subcarrier, then the SAP is detected by choosing the SAP with the maximum energy on the active subcarriers. For the tth group, the SAP is detected as

$$\hat{\mathcal{I}}^t = \underset{\forall\, \mathcal{I} \in \chi}{\arg\max} \left\{ \sum_i |\mathbf{y}^t(i)|^2, i \in \mathcal{A} \right\}, \tag{7}$$

where $\mathbf{y}^t$ denotes the tth subvector of $\mathbf{y}$, namely, the received signal of tth group, χ denotes the set of the SAPs, and $\mathcal{A}$ denotes the index of active subcarriers corresponding to the SAP $\mathcal{I}$. The computational complexity of energy detection is n complex multiplications and $N_{\mathcal{I}}k$ real additions for each group.

In the cascaded feedback detection, based on the detected SAP, the constellation symbols are detected as

$$\hat{\mathbf{s}} = \mathcal{D}\left(\mathbf{P}^H \bar{\mathbf{y}}(\hat{\mathcal{I}})\right), \tag{8}$$

where $\bar{\mathbf{y}}(\hat{\mathcal{I}})$ denotes the $N_1 \times 1$ subvector obtained from the $i \in \hat{\mathcal{I}}$ elements of $\bar{\mathbf{y}}$, $\mathcal{D}(\mathbf{P}^H \bar{\mathbf{y}}(\hat{\mathcal{I}}))$ denotes the vector of constellation symbols that are closest to the vector $\mathbf{P}^H \bar{\mathbf{y}}(\hat{\mathcal{I}})$. Noting that a unitary matrix is utilized as the precoder, we have $\mathbf{P}^{-1} = \mathbf{P}^H$, the operation of matrix inversion is avoided.

Based on the estimation of constellation symbols, the LCP is performed to obtain the symbols transmitted on the active subcarriers, which are given by

$$\mathbf{z} = \mathbf{P}\hat{\mathbf{s}} = [(\mathbf{z}^1)^T, (\mathbf{z}^2)^T, \cdots, (\mathbf{z}^G)^T]^T, \tag{9}$$

where $\mathbf{z}^t \in \mathbb{C}^{k\times 1}$ denotes the symbols conveyed on the active subcarriers of the tth group.

In this paper, the FFT matrix is adopted as the precoder to reduce complexity and improve the amplitude distribution of transmit signals [21], the complexity of precoding and deprecoding is just $\frac{N_1}{2}\log_2 N_1$ complex multiplications and $N_1 \log_2 N_1$ complex additions.

Then data-assisted SAP detection is performed group-by-group, and new SAP estimation is given by

$$\hat{\mathcal{I}}^t = \underset{\forall \mathcal{I}\in\chi}{\arg\min} \|\mathbf{y}^t - \mathbf{H}^t \gamma \mathbf{D}^t \mathbf{z}^t\|_2^2, \tag{10}$$

where $\mathbf{H}^t$ and $\mathbf{D}^t$ denote the tth submatrix of $\mathbf{H}$ and $\mathbf{D}$, respectively.

The new SAP estimation is generally more accurate than the last estimation result, and is used to refine the detection performance of the constellation symbols. In the data-assisted SAP detection, the constellation symbols are assumed to be known, the number of metric calculation in (10), is just $N_{\mathcal{I}}$ for each group.

Algorithm 1 Detection Algorithm

Input: $\mathbf{y}$,$\mathbf{H}$,$\mathbf{P}$
Output: $\hat{\mathcal{I}}$, $\hat{\mathbf{s}}$

1: MMSE equalization
$\bar{\mathbf{y}} = \Phi\mathbf{y}/\gamma$.
2: Energy detection
$\hat{\mathcal{I}}^t = \underset{\forall \mathcal{I}\in\chi}{\arg\max} \left\{\sum_i |\mathbf{y}^t(i)|^2, i \in \mathcal{A}\right\}$.
3: **for** $e = 1$ to e_{stop} **do**
4: Deprecding and symbol demodulation
$\hat{\mathbf{s}} = \mathcal{D}\left(\mathbf{P}^H \bar{\mathbf{y}}(\hat{\mathcal{I}})\right)$.
5: Linear precoding
$\mathbf{z} = \mathbf{P}\hat{\mathbf{s}} = [(\mathbf{z}^1)^T, (\mathbf{z}^2)^T, \cdots, (\mathbf{z}^G)^T]^T$.
6: Data-assisted SAP detection
$\hat{\mathcal{I}}^t = \underset{\forall \mathcal{I}\in\chi}{\arg\min} \|\mathbf{y}^t - \gamma\mathbf{H}^t\mathbf{D}^t\mathbf{z}^t\|_2^2$.
7: **end for**

The detection is summarized in Algorithm 1. The computational complexity of detection algorithm is evaluated in terms of the number of floating point operations (flops) per subcarrier. It is assumed that a flop can be either a real multiplication or real addition. Namely, a complex multiplication and a complex addition are counted as 6 flops and 2 flops, respectively. For convenience, we just consider the computational complexity of the cascaded feedback detection. The symbol demodulation $\mathcal{D}(c)$, which finds the constellation symbol that closest to the symbol c, is counted as $8M$ flops since a complex subtraction and a complex multiplication are performed for the calculation of the distance between the symbol c and each constellation symbol. The complexity of precoding or deprecoding is $5\ N_1 \log_2(N_1)$ flops, since the FFT matrix is used as the precoder. The complexity of data-assisted SAP detection is $N_{\mathcal{I}}(9n + 8k - 1)$ flops for each group. Hence, the total computational complexity of cascaded feedback detection is $e_{stop}\left(\gamma 8M + \gamma 10\log_2(N_1) + N_{\mathcal{I}}(9 + 8\gamma - 1/n)\right)$ flops/subcarrier. As shown in the simulation results, the value of e_{stop} can be set at two.

III. DIVERSITY ANALYSES

In this section, we show that energy detection can achieve the diversity order of $min(d/2, L)$, and a closed-form expression is derived for the energy detection, it is shown via the PEP analysis that the data-assisted SAP detection can achieve the diversity order of $min(d, L)$. For convenience and without confusion, we consider the signal of one group and the superscript is omitted in this section.

A. ENERGY DETECTION

Due to the fact that the elements of the CIR $\mathbf{h}_{\mathcal{T}}$ are independent and follows the complex Gaussian distribution, i.e., $\mathbf{h}_{\mathcal{T}} \sim \mathcal{CN}(0, 1/L)$, the element of the channel frequency response (CFR) $\mathbf{h} = \sqrt{N}\mathbf{F}_L\mathbf{h}_{\mathcal{T}}$ follows $\mathcal{CN}(0, \sigma_h^2)$, and $\sigma_h^2 = 1$.

The ith element of the received signal in the frequency domain is given by

$$\mathbf{y}(i) = \gamma\mathbf{h}(i)\mathbf{z}(i) + \mathbf{v}(i). \tag{11}$$

It is easy to see that the element of the received signal in the frequency domain follows complex Gaussian distribution, and

$$\mathbf{y}(i) \sim \begin{cases} \mathcal{CN}(0, \gamma^2\sigma_h^2\mathbf{z}(i)^2 + \sigma_v^2) & i \in \mathcal{A}, \\ \mathcal{CN}(0, \sigma_v^2) & i \notin \mathcal{A}. \end{cases} \tag{12}$$

Generally, we have $\gamma^2\sigma_h^2\mathbf{z}(i)^2 + \sigma_v^2 > \sigma_v^2$. Hence, for each group, the energy detection is given by

$$\hat{\mathcal{I}} = \underset{\forall \mathcal{I}}{\arg\max} \left\{\sum_i |\mathbf{y}(i)|^2, i \in \mathcal{A}\right\}. \tag{13}$$

Let X and Y denote the power of received signal for the inactive and active subcarriers, respectively. X and Y follow

the exponential distribution, and we yield

$$\begin{aligned} P(X > Y) &= \int_0^{+\infty} f_Y(Y) \int_0^{Y} f_X(X)\, dXdY, \\ &= \int_0^{+\infty} f_Y(Y) F_X(Y) dY, \\ &= \frac{\sigma_v^2}{2\sigma_v^2 + \gamma^2 z^2 \sigma_h^2}. \end{aligned} \tag{14}$$

where f_X and f_Y respectively denote the probability density function (PDF) of X and Y, F_X denotes the cumulative distribution function (CDF) of X, z denotes the signal on the active subcarriers.

After the LCP, we have $min(z^2) < 1$, the power of the constellation symbols is assumed to be unitary. Hence the LCP somewhat degrades the performance of energy detection. However, since the amplitude of the signal $\mathbf{z} = \mathbf{Ps}$ are different for the different realization of $\mathbf{s}$, and the statistical characteristic cannot be obtained. To achieve the closed-form expression, the impact of LCP is omitted, and we assumed that $\mathbf{y}(i) \sim \mathcal{CN}(0, \sigma_v^2), i \notin \mathcal{A}$ and $\mathbf{y}(i) \sim \mathcal{CN}(0, \gamma^2\sigma_h^2 + \sigma_v^2), i \in \mathcal{A}$. Namely, the OFDM-ISIM is considered here. As the LCP leads to the non-uniformity of the power of transmitted signal, which degrades the detection performance of energy detection, the closed-form expression derived in this section, can be regarded as a lower bound of the energy detection in the LCP-OFDM-ISIM.

B. DIVERSITY ANALYSIS FOR THE ENERGY DETECTION

For the energy detection, when the SAP $\mathcal{I}$ is erroneously detected as $\hat{\mathcal{I}}$, we have

$$\sum_{i\in\mathcal{A}} |\mathbf{y}(i)|^2 \leq \sum_{i\in\hat{\mathcal{A}}} |\mathbf{y}(i)|^2. \tag{15}$$

Since the minimum Hamming distance between $\mathcal{I}$ and $\hat{\mathcal{I}}$ is d, which is an even for the BCWC [19], the number of the distinct elements between $\mathcal{A}$ and $\hat{\mathcal{A}}$ is $r \geq d/2$. Let $\Delta_{\mathcal{A}}$ and $\Delta_{\hat{\mathcal{A}}}$ denote the r distinct elements in $\mathcal{A}$ and $\hat{\mathcal{A}}$, respectively. (15) can be simplified to r terms for analysis, and given by

$$\sum_{i\in\Delta_{\mathcal{A}}} |\mathbf{y}(i)|^2 \leq \sum_{i\in\Delta_{\hat{\mathcal{A}}}} |\mathbf{y}(i)|^2. \tag{16}$$

Since $\mathbf{y}(i)$ follows complex Gaussian distribution, $|\mathbf{y}(i)|^2$ follows the exponential distribution. Assuming that $\mathbf{h}(i), i \in \Delta_{\mathcal{A}}$ or $i \in \Delta_{\hat{\mathcal{A}}}$ are independent, since the interleaver is employed, as well as $\mathbf{y}(i), i \in \Delta_{\mathcal{A}}$ or $i \in \Delta_{\hat{\mathcal{A}}}$. Let $\mathcal{X}$ and $\mathcal{Y}$ denote $\sum_{i\in\Delta_{\hat{\mathcal{A}}}} |\mathbf{y}(i)|^2$ and $\sum_{i\in\Delta_{\mathcal{A}}} |\mathbf{y}(i)|^2$, respectively. Consequently, $\mathcal{X}$ and $\mathcal{Y}$ follow the Erlang distribution, and

$$\begin{aligned} \mathcal{X} &\sim Erlang(r, \frac{1}{\sigma_v^2}), \\ \mathcal{Y} &\sim Erlang(r, \frac{1}{\sigma_v^2 + \gamma^2\sigma_h^2}). \end{aligned} \tag{17}$$

where $Erlang(r, \lambda)$ denotes the Erlang distribution with shape parameter r and rate parameter λ.

Let us define $\lambda_{\mathcal{X}} = 1/\sigma_v^2$ and $\lambda_{\mathcal{Y}} = 1/(\sigma_v^2 + \gamma^2\sigma_h^2)$. The probability of the pairwise error event $\mathcal{I} \to \hat{\mathcal{I}}$ is given by

$$\begin{aligned} &P(\mathcal{I} \to \hat{\mathcal{I}}) \\ &= P(\mathcal{X} \geq \mathcal{Y}) = \int_0^{+\infty} F_{\mathcal{Y}}(\mathcal{X}) f_{\mathcal{X}}(\mathcal{X}) d\mathcal{X}, \\ &= 1 - \sum_{n=0}^{r-1} \frac{1}{n!(r-1)!} \lambda_{\mathcal{X}}^r \lambda_{\mathcal{Y}}^n \frac{(n+r-1)!}{(\lambda_{\mathcal{X}} + \lambda_{\mathcal{Y}})^{n+r}}, \\ &= 1 - \sum_{n=0}^{r-1} \frac{1}{n!(r-1)!} \lambda_{\mathcal{X}}^r \lambda_{\mathcal{Y}}^n \frac{(n+r-1)!}{\sum_{i=0}^{n+r} C_{n+r}^i \lambda_{\mathcal{X}}^i \lambda_{\mathcal{Y}}^{n+r-i}}, \\ &= 1 - \sum_{n=0}^{r-1} \frac{1}{n!(r-1)!} \lambda_{\mathcal{X}}^r \lambda_{\mathcal{Y}}^n \frac{(n+r-1)!}{\sum_{i=0}^{n+r} \frac{(n+r)!}{i!} \lambda_{\mathcal{X}}^i \lambda_{\mathcal{Y}}^{n+r-i}}, \\ &= 1 - \sum_{n=0}^{r-1} \frac{1}{n!(r-1)!} \frac{1}{(n+r)\sum_{i=0}^{n+r} \frac{1}{i!} \lambda_{\mathcal{X}}^{i-r} \lambda_{\mathcal{Y}}^{r-i}}, \\ &= 1 - \sum_{n=0}^{r-1} \left(n!(r-1)!(n+r) \sum_{i=0}^{n+r} \frac{1}{i!} \left(\frac{\lambda_{\mathcal{Y}}}{\lambda_{\mathcal{X}}} \right)^{r-i} \right)^{-1}. \end{aligned} \tag{18}$$

where $f_{\mathcal{X}}(\mathcal{X})$ and $F_{\mathcal{Y}}(\mathcal{X})$ denote the PDF and CDF of $\mathcal{X}$ and $\mathcal{Y}$, respectively, and are given by

$$f_{\mathcal{X}}(\mathcal{X}) = \frac{\lambda_{\mathcal{X}}^r \mathcal{X}^{r-1} \exp(-\lambda_{\mathcal{X}}\mathcal{X})}{(r-1)!}. \tag{19}$$

$$F_{\mathcal{Y}}(\mathcal{X}) = 1 - \sum_{n=0}^{r-1} \frac{1}{n!} \exp(-\lambda_{\mathcal{Y}}\mathcal{X})(\lambda_{\mathcal{Y}}\mathcal{X})^n. \tag{20}$$

Due to the fact that $\lambda_{\mathcal{Y}} > \lambda_{\mathcal{X}}$, it is obvious that the detection performance of energy detection improves with the increasing of r. Noting that the upper bound of the number of the independent channel coefficients is L for L-taps channel, and the maximum of the number of the independent elements in $\mathbf{h}(i), i \in \Delta_{\hat{\mathcal{A}}}$ or $i \in \Delta_{\mathcal{A}}$ is L. Hence the maximum achievable diversity order is L for L-taps channel, and (18) provides a closed-form expression for the energy detector when the diversity order of r is achieved by the SAP with the minimum Hamming distance of r. When the SAP with the minimum Hamming distance of $d > 2L$ is employed for L-taps channel, the detection performance will be much poor than the value of (18), since the maximum achievable diversity order is L for L-taps channel. Hence the diversity order of energy detection is $r = min(d/2, L)$, for L-taps channel, conditioned on the BCWC with the minimum Hamming distance d.

When the diversity order of r is achieved by the BCWC with the minimum Hamming distance of $d = 2r$, the average bit error probability (ABEP) of the energy detection is given by

$$P_e = \frac{1}{pn_{\mathcal{I}}} \sum_{\mathcal{I}} \sum_{\hat{\mathcal{I}}} P(\mathcal{I} \to \hat{\mathcal{I}}) e(\mathcal{I}, \hat{\mathcal{I}}), \tag{21}$$

where p denotes the number of the bits conveyed by the SAP, $n_{\mathcal{I}}$ is the number of the possible realizations of $\mathcal{I}$, $e(\mathcal{I}, \hat{\mathcal{I}})$ represents the number of the bit errors for the corresponding pairwise error event.

According to the (21), the Gray-mapping should be adopted for the SAP labeling to optimize the performance. Namely, the lager of the Hamming distance between $\mathcal{I}$ and $\hat{\mathcal{I}}$, the larger value of $e(\mathcal{I}, \hat{\mathcal{I}})$.

C. DIVERSITY ANALYSIS FOR THE DATA-ASSISTED SAP DETECTION

Since the estimated constellation symbols are linear precoded again and used in the data-assisted SAP detection, and by the LCP, the error estimation of the constellation symbols can be regarded as the additional noise for the data-assisted SAP detection [22], [23], we assume that the symbols are known in the following diversity analysis for the data-assisted SAP detection.

For the data-assisted SAP detection, if the SAP $\mathcal{I}$ is erroneously detected as $\hat{\mathcal{I}}$, we have

$$||\mathbf{y} - \gamma\mathbf{H}\mathbf{D}\mathbf{z}||_2^2 \geq ||\mathbf{y} - \gamma\mathbf{H}\hat{\mathbf{D}}\mathbf{z}||_2^2, \tag{22}$$

where $\mathbf{D}$ and $\hat{\mathbf{D}}$ are the data permutation matrices corresponding to the $\mathcal{I}$ and $\hat{\mathcal{I}}$, respectively, $\mathbf{z}$ is the symbols conveyed on the active subcarriers.

The corresponding PEP of $\mathcal{I} \to \hat{\mathcal{I}}$ is given by

$$\begin{aligned} P(\mathcal{I} \to \hat{\mathcal{I}}|\mathbf{h}) &= P\left(||\mathbf{y} - \gamma\mathbf{H}\mathbf{D}\mathbf{z}||_2^2 \geq ||\mathbf{y} - \gamma\mathbf{H}\hat{\mathbf{D}}\mathbf{z}||_2^2\right), \\ &= Q\left(\sqrt{\frac{\|\gamma\mathbf{H}(\mathbf{D} - \hat{\mathbf{D}})\mathbf{z}\|_2^2}{2\sigma_v^2}}\right), \\ &\leq Q\left(\sqrt{\frac{\gamma^2 \sum_{i\in\Delta_{\mathcal{I}}} |\mathbf{h}(i)\mathbf{z}(i)|^2}{2\sigma_v^2}}\right), \end{aligned} \tag{23}$$

where $\Delta_{\mathcal{I}}$ denotes the ordering of $r_1 \geq d$ distinct elements between $\mathcal{I}$ and $\hat{\mathcal{I}}$. Let $\vec{\Delta}_{\mathcal{I}}$ denote the ordering of the $i \in \Delta_{\mathcal{I}}$ subcarriers before the de-interleaving in the block, we yield

$$\begin{aligned} \sum_{i\in\Delta_{\mathcal{I}}} |\mathbf{h}(i)\mathbf{z}(i)|^2 &\leq z_{min}^2 \sum_{i\in\vec{\Delta}_{\mathcal{I}}} \mathbf{h}_{\mathcal{T}}^H \mathbf{F}_L^H(i,:)\mathbf{F}_L(i,:)\mathbf{h}_{\mathcal{T}}, \\ &= z_{min}^2 \mathbf{h}_{\mathcal{T}}^H \left(\sum_{i\in\vec{\Delta}_{\mathcal{I}}} \mathbf{F}_L^H(i,:)\mathbf{F}_L(i,:)\right)\mathbf{h}_{\mathcal{T}}, \\ &= z_{min}^2 \mathbf{h}_{\mathcal{T}}^H \left(\sum_{i\in\vec{\Delta}_{\mathcal{I}}} \mathbf{A}_i\right)\mathbf{h}_{\mathcal{T}}, \\ &= z_{min}^2 \mathbf{h}_{\mathcal{T}}^H \mathbf{A}\mathbf{h}_{\mathcal{T}}, \end{aligned} \tag{24}$$

where z_{min}^2 denotes the minimum value of $|\mathbf{z}(i)|^2, i \in \Delta_{\mathcal{I}}$, $\mathbf{A}_i$ is a $L \times L$ matrix with rank one, and the rank of the matrix $\mathbf{A}$ is given by $rank(\mathbf{A}) = min(r_1, L)$. (The proof can be found in the appendix in [24]). Considering the fact that $\mathbf{A}_i$ is positive semidefinite Hermitian, as well as $\mathbf{A}$, we can decompose $\mathbf{A}$ as

$$\mathbf{A} = \mathbf{U}\Lambda\mathbf{U}^H, \tag{25}$$

where $\mathbf{U}$ is an $L \times L$ unitary matrix, and Λ is an $L \times L$ diagonal matrix, whose diagonal vector is the eigenvalues of $\mathbf{A}$, $\lambda_i(\mathbf{A}), i = 0, \cdots, L-1$ in decreasing order.

Let us denote the vector $\mathbf{U}\mathbf{h}_{\mathcal{T}}$ by $\mathbf{u}$, (23) is rewritten as

$$\begin{aligned} &P(\mathcal{I} \to \hat{\mathcal{I}}) \\ &\leq E\left\{Q\left(\sqrt{\frac{\gamma^2 \sum_{i\in\Delta_{\mathcal{I}}} |\mathbf{h}(i)\mathbf{z}(i)|^2}{2\sigma_v^2}}\right)\right\}, \\ &\leq E\left\{\exp\left(\frac{\gamma^2 z_{min}^2 \sum_{i=0}^{L-1} \lambda_i(\mathbf{A})|\mathbf{u}(i)|^2}{4\sigma_v^2}\right)\right\}, \\ &= \prod_{i=0}^{L-1}\left(1 + \frac{\gamma^2 z_{min}^2 \lambda_i(\mathbf{A})}{4\sigma_v^2}\right)^{-1}, \\ &\approx \left(\prod_{i=0}^{min(r_1,L)-1} \lambda_i(\mathbf{A})\right)^{-1} \left(\frac{\gamma^2 z_{min}^2}{4\sigma_v^2}\right)^{-min(r_1,L)}. \end{aligned} \tag{26}$$

As shown in (26), the data-assisted SAP detection achieves the diversity order of $min(r_1, L) = min(d, L)$ for the information conveyed by the SAPs. Similar as in the energy detection, the LCP also degrades the performance of data-assisted SAP detection, since we have the value of $z_{min}^2 < 1$ when the LCP is employed. However since the power of inactive subcarriers is relocated on the active subcarriers in the LCP-OFDM-ISIM, the power gain (corresponding to the factor γ^2) is achieved and can somewhat compensate the performance loss. Further, we can choose a BCWC with greater the minimum Hamming distance $d > L$ to achieve additional coding gain to improve the performance of the LCP-OFDM-ISIM.

IV. SIMULATION RESULTS

In this section, the simulation results are provided to testify our conclusions and evaluate the performance of the proposed LCP-OFDM-ISIM. We first show the detection performance of energy detection for the SAP with different the minimum Hamming distance. Then, we present the performance of the proposed cascaded feedback detection for the LCP-OFDM-ISIM. Finally, we compare the LCP-OFDM-ISIM with the CI-OFDM-IM [13], ECI-OFDM-IM [14], LCP-OFDM [25], and S-OFDM-IM [16].

A. PERFORMANCE OF ENERGY DETECTION

In this subsection, we compare the simulation results with the values in (21) to testify our analyses for the energy detection, and show that the energy detection can achieve the diversity order of $min(d/2, L)$. In the simulation, the OFDM-ISIM employing the BPSK is considered. The number of the subcarriers in a block is $N = 192$, the channel order is $L = 4$, the interleaving depth is $N/L = 48$.

As shown in Table. 3, the minimum Hamming distance of the SAP for $(n, k) = (2, 1)$ is $d = 2$. For convenience, repetition code is used to generate the SAP with different the minimum Hamming distance. For example, the SAP in Table. 3 is repeated twice to generate the SAP with the minimum Hamming distance of $d = 4$, provided in Table. 2.

As shown in Fig. 2, the performance of energy detection is significantly improved with the increasing of repetition rate

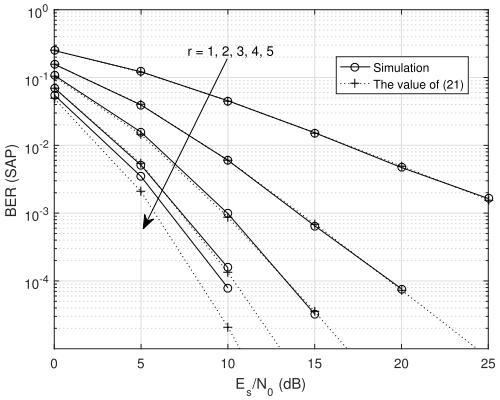

FIGURE 2. Performance of energy detection for the OFDM-ISIM employing the SAP with different the minimum Hamming distance.

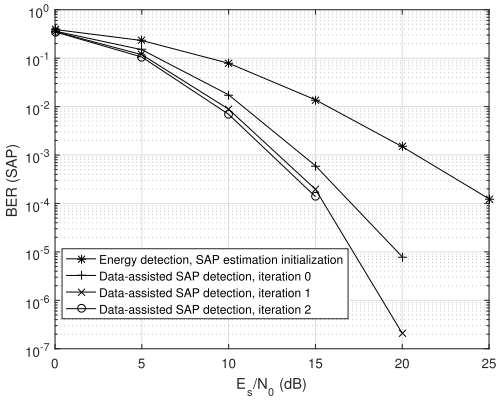

FIGURE 3. BER Performance of the LCP-OFDM-ISIM with different iteration detection, for the information conveyed by the SAPs.

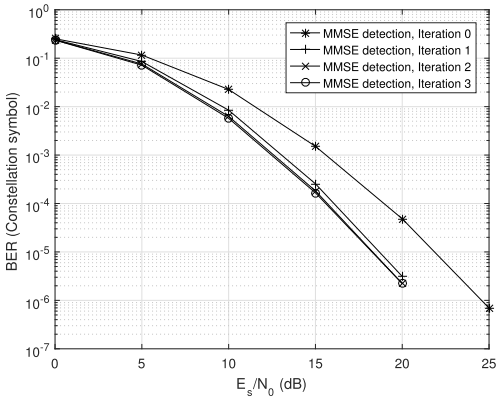

FIGURE 4. BER Performance of the LCP-OFDM-ISIM with different iteration detection, for the information conveyed by the constellation symbols.

(or the minimum Hamming distance between two SAPs), and the simulation results are coherent with the value of (21), when $r = 1, 2, 3, 4$. It is notable that when the repetition rate is set to be $r = 5$, the simulation result is poorer than the value of (21) with $r = 5$, this is because that the values of (21) with $r = 5$ provides the performance of energy detection with diversity order of five, however the maximum achievable frequency diversity order is four for the $L = 4$-taps channel. Hence r is even set at five, the simulation results still achieves the diversity order of four. It is also found that when $r = 5$, the simulation result is better than the value of (21) with $r = 4$, this is because that a greater coding gain is achieved when r changes from four to five.

B. PERFORMANCE OF CASCADED FEEDBACK DETECTION

In this subsection, we show the performance of the LCP-OFDM-ISIM with the cascaded feedback detection. The value of (n, k) is set to be $(16, 12)$, and binary-phase shift keying (BPSK) is employed. The channel order is $L = 6$, the interleaving depth is $N/n = 12$. The SAPs, with cardinality $N_{\mathcal{I}} = 16$, are chosen from the BCWC $A(16, 6, 12)$ [19] to achieve the diversity order of six for the information conveyed by the SAPs and convey four bits for each group.

As shown in Fig. 3 and Fig. 4, for the information conveyed by both the constellation symbols and SAPs, the detection performances are significantly improved by the cascaded feedback detection. For the information conveyed by the SAPs, since the energy detection just achieves the diversity order of $d/2 = 3$, the data-assisted SAP detection can achieve the diversity order of $d = 6$, the detection performance is significantly improved by the first iteration. Due to the fact that the detection performance of the constellation symbols depends on the detection performance of the SAPs, the detection performance of the constellation symbols is also significantly improved by the first iteration. It is notable that the performance of SAP detection is much improved by the second iteration, however the performance improvement of constellation symbol detection is slight. This is because that the LCP degrades the dependence of the constellation symbol detection on the SAP detection. In the LCP-OFDM-ISIM, the error SAP detection just leads to the data distortion for the constellation symbol detection, rather than the error constellation symbol detection like in the OFDM-IM. As seen from the Fig. 3 and Fig. 4, the performance of the LCP-OFDM-ISIM almost remains the same after the first iteration. Hence, the value of e_{stop} can be set at two in cascaded feedback detection. For convenience, only the results of the first iteration are presented in the following performance comparison.

C. PERFORMANCE COMPARISON

In this subsection, we compare the performance of the LCP-OFDM-ISIM with the performance of CI-OFDM-IM, ECI-OFDM-IM, LCP-OFDM, and S-OFDM-IM. The block length and channel order are $N = 192$ and $L = 6$, respectively. The interleaving depth is $N/n = 12$. According to the study in [13], the constellation rotation angle of CI-OFDM-IM is set to be 45 and 15 degrees for the BPSK and four-ary quadrature amplitude modulation (4-QAM), respectively. According the study in [14], the rotation angle of ECI-OFDM-IM is 10 degrees. For the CI-OFDM-IM and

ECI-OFDM-IM, the LLR of the subcarrier is active to inactive, is first calculated, the SAP is detected by choosing the SAP with the maximum LLR value, then the constellation symbols are detected by the ML detection. For the LCP-OFDM, the MMSE equalization is first performed, then the deprecoding and symbol-by-symbol decision are performed in a sequence, like in the LCP-OFDM-ISIM.

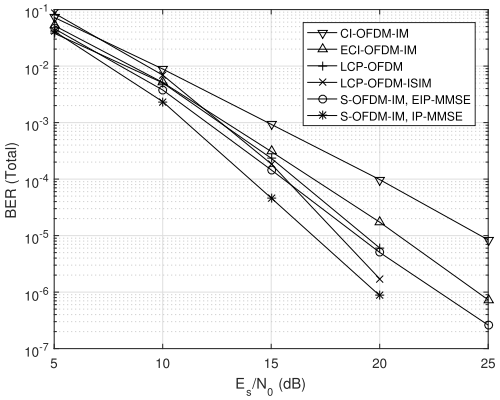

FIGURE 5. BER performance of CI-OFDM-IM, ECI-OFDM-IM, LCP-OFDM, LCP-OFDM-ISIM, and S-OFDM-IM, for the SE of 1 bps/Hz.

In Fig. 5, we compare the LCP-OFDM-ISIM with the benchmarks for the SE of 1 bps/Hz. The BPSK is employed for all the schemes. The BCWC $A(16, 6, 12)$ is utilized as the SAP for the CI-OFDM-IM, ECI-OFDM-IM, and LCP-OFDM-ISIM, the number of the valid SAPs is $N_{\mathcal{I}} = 16$, four bits are conveyed by the SAP for each group. According to the study in [16], the group length should be greater than the channel order to achieve the diversity for S-OFDM-IM. Furthermore, to make the power gain of CI-OFDMIM, ECI-OFDM-IM, LCP-OFDM-ISIM, and S-OFDM-IM be the same, namely, the same value of γ is achieved for the four schemes, the BCWC $A(8, 4, 6)$ is utilized as the SAP for S-OFDM-IM, the number of the valid SAPs is $N_{\mathcal{I}} = 4$, two bits are conveyed by the SAP for each group.

As seen from Fig. 5, ECI-OFDM-IM achieves a better performance than CI-OFDM-IM due to a higher diversity order. Even the MMSE equalization is employed, the LCP-OFDM and LCP-OFDM-ISIM achieves a better performance than ECI-OFDM-IM and CI-OFDM-IM. It is notable that the performance gap between the LCP-OFDM and ECI-OFDM-IM is much less than the performance gap between the ECI-OFDM-IM and CI-OFDM-IM, this is because that the LCP-OFDM-ISIM and LCP-OFDM employ the MMSE detection, however the CI-OFDM and ECI-OFDM-IM employ the ML detection for the constellation symbol detection. The performance of LCP-OFDM-ISIM is better than the S-OFDM-IM employing EIP-MMSE detection, while worsen than the S-OFDM-IM employing IP-MMSE detection. However the complexity order of S-OFDM-IM employing IP-MMSE, in terms of flops per subcarrier, is $\mathcal{O}(N_{\mathcal{I}}k^2)$, which is much higher than the complexity of the cascaded feedback detection in LCP-OFDM-ISIM. Further, the LCP-OFDM-ISIM achieves a better performance than LCP-OFDM in the high-SNR conditions, since the power of inactive subcarriers is relocated on the active subcarriers in the LCP-OFDM-ISIM, the power gain is achieved. It is also notable that the performance of the LCP-OFDM-ISIM is poor in the low-SNR conditions, this is because that after the LCP, the amplitude of the symbols is no longer unitary, the minimum value, i.e., z_{min} may be very small and close to zero, which degrades the performance of SAP detection.

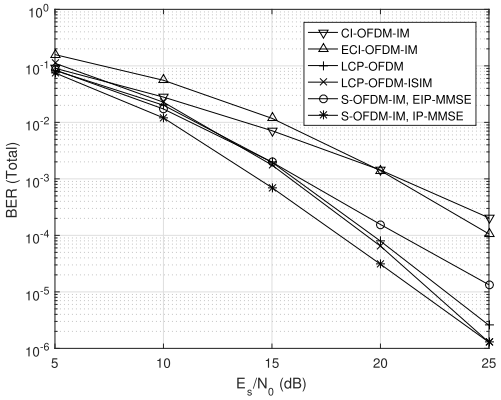

FIGURE 6. BER performance of CI-OFDM-IM, ECI-OFDM-IM, LCP-OFDM, LCP-OFDM-ISIM, and S-OFDM-IM, for the SE of 1.625 bps/Hz.

In Fig. 6, we compare the LCP-OFDM-ISIM with the benchmarks for the SE of 1.625 bps/Hz. The 4-QAM is employed for all the schemes. As shown in Fig. 5, the performance of LCP-OFDM-ISIM is poor in the low-SNR conditions, in this simulation, the BCWC with greater the minimum Hamming distance $d > L$ is utilized as the SAP to improve the performance of LCP-OFDM-ISIM. The BCWC $A(24, 8, 18)$ is utilized as the SAP for the CI-OFDM-IM, ECI-OFDM-IM, and LCP-OFDM-ISIM. The number of the valid SAPs is $N_{\mathcal{I}} = 8$, four bits are conveyed by the SAP for each group. For the S-OFDM-IM, the BCWC $A(8, 4, 6)$ is utilized as the SAP, the number of the valid SAPs is $N_{\mathcal{I}} = 2$, one bits are conveyed by the SAP for each group. The same power gain is also achieved for the four schemes.

For the fair of comparison and achieving the SE of 1.625 bps/Hz for LCP-OFDM, similar as in [17] , $13N/16$ subcarriers (namely, 156 out of $N = 192$ subcarriers) are randomly activated to convey the symbols, the power of the inactive subcarriers is relocated on the active subcarriers, however the SAP is known at the receiver and is not exploited to convey additional information.

As shown in Fig. 6, since the LCP-OFDM-ISIM employs the BCWC with the minimum Hamming distance of eight is utilized as the SAP for $L = 6$-taps channel, the performance of LCP-OFDM-ISIM is much improved. Especially in low-SNR conditions, the LCP-OFDM-ISIM achieves a better performance than CI-OFDM and ECI-OFDM-IM. It is notable that in the low-SNR conditions, CI-OFDM-IM achieves a better performance than ECI-OFDM-IM performance, this is because that ECI is no longer an orthogonal

design, the single-symbol ML decoding property of CI orthogonal design is absent for the ECI. Consequently, the ECI achieves a higher diversity order at the cost of Euclidean distance between the symbols in comparison with CI. Comparing with the ECI-OFDM-IM, the proposed LCP-OFDM-ISIM achieves diversity, further, the Euclidean distance between the symbols is unchanged before and after the LCP, since a unitary matrix is adopted as the precoder. Specially, the LCP-OFDM-ISIM achieves almost the same performance with the S-OFDM-IM employing IP-MMSE detection in the high-SNR conditions, this is because that the BCWC with greater the minimum Hamming distance is utilized as SAP for the LCP-OFDM-ISIM, the SAP detection is much improved.

V. CONCLUSION

LCP-OFDM-ISIM has been proposed in this paper, where a unitary matrix is used to spread the constellation symbols over all the active subcarriers of the block, and the BCWC is utilized as the SAP. To make the detection of LCP-OFDM-ISIM with performable complexity, the SAP is first estimated by the energy detection, which achieves the diversity order of $min(d/2, L)$, then the cascaded feedback detection is proposed to refine the detection performance by passing the detection results between the symbol detection and data-assisted SAP detection. It is shown via the PEP analysis that the data-assisted SAP detection can achieve the diversity order of $min(L, d)$. Simulation results show that the proposed LCP-OFDM-ISIM is an effective scheme to improve the performance of OFDM-IM with practical complexity.

REFERENCES

[1] E. Başar, U. Aygölü, E. Panayirci, and H. V. Poor, "Orthogonal frequency division multiplexing with index modulation," *IEEE Trans. Signal Process.*, vol. 61, no. 22, pp. 5536–5549, Nov. 2013.

[2] E. Başar, "Index modulation techniques for 5G wireless networks," *IEEE Commun. Mag.*, vol. 54, no. 7, pp. 168–175, Jul. 2016.

[3] Q. Li, M. Wen, H. V. Poor, and F. Chen, "Information guided precoding for OFDM," *IEEE Access*, vol. 5, pp. 19644–19656, 2017.

[4] T. Mao, Q. Wang, Z. Wang, and S. Chen, "Novel index modulation techniques: A survey," *IEEE Commun. Surveys Tuts.*, vol. 21, no. 1, pp. 315–348, 1st Quart., 2018.

[5] R. Fan, Y. J. Yu, and Y. L. Guan, "Generalization of orthogonal frequency division multiplexing with index modulation," *IEEE Trans. Wireless Commun.*, vol. 14, no. 10, pp. 5350–5359, Oct. 2015.

[6] M. Wen, B. Ye, E. Basar, Q. Li, and F. Ji, "Enhanced orthogonal frequency division multiplexing with index modulation," *IEEE Trans. Wireless Commun.*, vol. 16, no. 7, pp. 4786–4801, Jul. 2017.

[7] T. Mao, Z. Wang, Q. Wang, S. Chen, and L. Hanzo, "Dual-mode index modulation aided OFDM," *IEEE Access*, vol. 5, pp. 50–60, 2017.

[8] Q. Li, M. Wen, E. Basar, H. V. Poor, B. Zheng, and F. Chen, "Diversity enhancing multiple-mode OFDM with index modulation," *IEEE Trans. Commun.*, vol. 66, no. 8, pp. 3653–3666, Aug. 2018.

[9] S. Lu, I. A. Hemadeh, M. El-Hajjar, and L. Hanzo, "Compressed-sensing-aided space-time frequency index modulation," *IEEE Trans. Veh. Technol.*, vol. 67, no. 7, pp. 6259–6271, Jul. 2018.

[10] J. Choi, "Noncoherent OFDM-IM and its performance analysis," *IEEE Trans. Wireless Commun.*, vol. 17, no. 1, pp. 352–360, Jan. 2018.

[11] S. Althunibat, R. Mesleh, and E. Basar, "Differential subcarrier index modulation," *IEEE Trans. Veh. Technol.*, vol. 67, no. 8, pp. 7429–7436, Aug. 2018.

[12] Y. Xiao, S. Wang, L. Dan, X. Lei, P. Yang, and W. Xiang, "OFDM with interleaved subcarrier-index modulation," *IEEE Commun. Lett.*, vol. 18, no. 8, pp. 1447–1450, Aug. 2014.

[13] E. Başar, "OFDM with index modulation using coordinate interleaving," *IEEE Wireless Commun. Lett.*, vol. 4, no. 4, pp. 381–384, Aug. 2015.

[14] Y. Liu, F. Ji, H. Yu, F. Chen, D. Wan, and B. Zheng, "Enhanced coordinate interleaved OFDM with index modulation," *IEEE Access*, vol. 5, pp. 27504–27513, 2017.

[15] J. Choi, "Coded OFDM-IM with transmit diversity," *IEEE Trans. Commun.*, vol. 65, no. 7, pp. 3164–3171, Jul. 2017.

[16] T. Van Luong and Y. Ko, "Spread OFDM-IM with precoding matrix and low-complexity detection designs," *IEEE Trans. Veh. Technol.*, vol. 67, no. 12, pp. 11619–11626, Dec. 2018.

[17] H. Zhang, C. Jiang, L.-L. Yang, E. Basar, and L. Hanzo, "Linear precoded index modulation," *IEEE Trans. Commun.*, vol. 67, no. 1, pp. 350–363, Jan. 2019.

[18] Z. Yang, F. Chen, B. Zheng, M. Wen, and W. Yu, "Carrier frequency offset estimation for OFDM with generalized index modulation systems using inactive data tones," *IEEE Commun. Lett.*, vol. 22, no. 11, pp. 2302–2305, Nov. 2018.

[19] A. E. Brouwer, J. B. Shearer, N. J. A. Sloane, and W. D. Smith, "A new table of constant weight codes," *IEEE Trans. Inf. Theory*, vol. 36, no. 6, pp. 1334–1380, Nov. 1990.

[20] P. R. J. Ostergard, "Classification of binary constant weight codes," *IEEE Trans. Inf. Theory*, vol. 56, no. 8, pp. 3779–3785, Aug. 2010.

[21] A. Bury, J. Egle, and J. Lindner, "Diversity comparison of spreading transforms for multicarrier spread spectrum transmission," *IEEE Trans. Commun.*, vol. 51, no. 5, pp. 774–781, May 2003.

[22] K. C. Chan, W. C. Huang, C. P. Li, and H. J. Li, "Elimination of data identification problem for data-dependent superimposed training," *IEEE Trans. Signal Process.*, vol. 63, no. 6, pp. 1595–1604, Mar. 2015.

[23] G. Dou, C. He, C. Li, and J. Gao, "Channel estimation and symbol detection for OFDM systems using data-nulling superimposed pilots," *Electron. Lett.*, vol. 50, no. 3, pp. 179–180, Jan. 2014.

[24] E. Akay and E. Ayanoglu, "Achieving full frequency and space diversity in wireless systems via BICM, OFDM, STBC, and Viterbi decoding," *IEEE Trans. Commun.*, vol. 54, no. 12, pp. 2164–2172, Dec. 2006.

[25] Z. Liu, X. Yan, and G. B. Giannakis, "Linear constellation precoding for OFDM with maximum multipath diversity and coding gains," *IEEE Trans. Commun.*, vol. 51, no. 3, pp. 416–427, Mar. 2003.

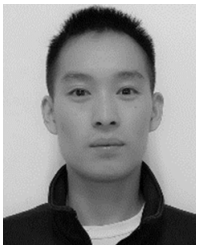

QINGBO WANG received the B.S. degree from Hunan University (HNU), in 2014, and the M.S. degree from the Naval University of Engineering (NUE), China, in 2016, where he is currently pursuing the Ph.D. degree. His research interests include the areas of channel estimation, index modulation, and cooperative communication.

GAOQI DOU received the B.S. and Ph.D. degrees in communication engineering from the Naval University of Engineering (NUE), China, in 2004 and 2009, respectively, where he is currently an Associate Professor with the Department of Communication Engineering. His research interests include the areas of channel estimation, cooperative communication, and coding theory.

JUN GAO received the M.S. and Ph.D. degrees from the Beijing Institute of Technology (BIT), in 1986 and 1989, respectively. He is currently a Professor with the Department of Communication Engineering, Naval University of Engineering (NUE). His research interest includes the area of wireless communication, with an emphasis on digital signal process and coding theory.

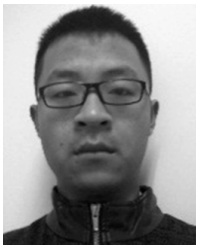

RAN DENG received the B.S. degree from the Huazhong University of Science and Technology, in 2013, and the M.S. degree from the Naval University of Engineering (NUE), China, in 2015, where he is currently pursuing the Ph.D. degree. His research interests include the areas of channel estimation, cooperative communication, and interference cancellation.